A Surface Division Method of Parts Mesh Model for On-Machine Inspection

XINCHENG LU, BUYUN SHENG, HUI WANG, RUIPING LUO, GAOCAI FU, AND QIBING LU

School of Mechanical and Electronic Engineering, Wuhan University of Technology, Wuhan 430070, China
Hubei Digital Manufacturing Key Laboratory, Wuhan University of Technology, Wuhan 430070, China

Corresponding author: Buyun Sheng (shengby@whut.edu.cn)

ABSTRACT As a general 3D model data format, triangular mesh model has been widely used in mechanical engineering to realize the function of transmitting data between different CAD software, but during the transmission, a large amount of geometric and topological data from mechanical parts has been lost. In order to solve this problem while using triangular mesh model in On-Machine Inspection (OMI), in this paper, a surface division method of parts mesh model for OMI is proposed, intending to solve the problem about mesh model that divided into triangular pieces cannot be operated during OMI. The proposed method contains two processes: boundary line extraction and mesh model division. During the process of extracting boundary line of model surface, a method of extracting coordinate points on the model boundary is proposed by analyzing the Gauss curvature between triangular surfaces, and then using the maximum entropy threshold theory to analyze the correlation between coordinate points to screen out the qualified model boundary line. In the process of mesh model division, based on the extracted model boundary, a mesh segmentation method based on region - growing algorithm is studied to obtain the triangular mesh within the boundary. At last, the validity of the described method is verified by some example.

I. INTRODUCTION

The rapid development of manufacturing industry makes the position of precision measurement technology in the field of mechanical manufacturing increasingly prominent, but also makes the machine inspection as a new high-efficiency detection method gradually widely used [1], On-Machine Inspection (OMI) system can carry out quality inspection with high-efficiency of mechanical parts without moving parts. However, with the increasing variety of parts in some mechanical fields, the geometric expression of parts is becoming more complicated, data transmission and sharing are becoming more difficult. To solve this problem digital geometry processing technology based on triangular mesh model has gradually become a research hotspot in the field of computer aided design and manufacturing in recent years [2], in which triangular mesh segmentation is the basis of mesh model processing in OMI process [3], [4].

As an approximation to the real model, the triangular mesh model has characteristics of simple data structure, small file size and strong universal property. However, the original triangular mesh model does not have topological information, so the operator cannot perform any complex operation on the model surface during OMI. To achieve this purpose, it is necessary to accurately segment the triangular mesh model of parts. In most cases, the model mesh segmentation process some objects such as toys, tables, chairs, cup and bowl containers et.al have no strict boundary distinction. The actual partition process is to divide the model into multiple blocks that conform to people's cognition. The accuracy of block boundary has little effect on the model [5]–[7]. But most mechanical parts have clear boundary, which needs to be searched by combining the geometric properties of parts themselves in the process of model segmentation, and the accuracy of boundary segmentation results will directly affect the subsequent operation and analysis of mesh model. Therefore, study the surface division of part triangular mesh model will be beneficial to the analysis and processing of part model during OMI, these processing processes include the

The associate editor coordinating the review of this manuscript and approving it for publication was Zhixiong Peter Li.

inspection part selection of mechanical part, the distribution of measuring points on model surface, and the path planning of measurement process. All of them are related to the part triangular mesh model and require the grid model data possess the corresponding geometry and topology information.

In view of the above analysis, in order to realize the processing of part mesh model during OMI, this paper presents a surface division method of parts mesh model for OMI. The purpose of this method is to solve the problem that the corresponding geometric features and topology information cannot be obtained when using the triangular mesh model during OMI. The main contributions of this paper are as follows: (1) We combined three methods to realize the fast automatic partition of geometric surface on the triangular mesh model of mechanical parts, they are the calculation method of Gaussian curvature, the model boundary line extraction method based on maximum between-cluster variance and the region growth algorithm for triangular plane in boundary. (2) We determined the threshold of Gaussian curvature on boundary line by the two-dimensional maximum entropy threshold method. Using the two-dimensional maximum entropy threshold to analyze the Gaussian curvature at each coordinate point of triangular mesh model, to find out the boundary between data sets, as the threshold to divide the curvature data, to realize the rapid extraction of boundary points on triangular mesh model. (3) We process the extracted boundary points and obtain the corresponding boundary line, calculate the angle of plane which formed the boundary line, then obtain the threshold value of boundary determination by the method of maximum between-cluster variance, so that we can extract boundary data on the model. (4) We combined the theory of ant colony algorithm and Monte Carlo tree search algorithm to do the close test for extracted boundary, and correct the incomplete boundary by extending the boundary at the breakpoint, it helps to improve the accuracy and credibility of results. (5) Based on the principle of the region growth algorithm and the boundary line extracted from the triangular mesh model, we extract and classify the triangular surface slices within the boundary line partition range, and reconstruct the geometric topology structure of triangular mesh model surface. This method accurately and completely divides the disordered triangular surface in the model, provides convenience for the subsequent analysis operation on the part model, realizes the operability of the part triangular mesh model and provides support for the OMI of mechanical products.

II. RELATED WORK

At present, the triangular mesh model segmentation has developed from the early artificial segmentation to automatic segmentation, researchers have proposed many effective methods. Quirita *et al.* [8] proposed a special region growth method called multiresolution-region-growing segmentation, which can avoid falling into the local minimum by specifying multiple seed elements of triangular mesh model, but is slow in obtaining the optimal solution. Zhang *et al.* [5] proposed a 3D shape hierarchical segmentation method, based on the

splats similarity measure index, which automatically generates the hierarchical structure of the segmentation region through adaptive clusters. The result shows that segmentation effect of CAD model and the triangular mesh model reconstructed by point cloud is good. Yang *et al.* [9] proposed a fast mesh segmentation method based on modified region growth algorithm. By detecting the dihedral angle extraction feature lines of the non-boundary edge triangles and make it as boundary constraint for region growth process, the problem of over-segmentation was solved. Venu Bitla *et al.* [10] developed standard data access interface for high-level surface features such as B spline that preserved as general STEP model files (AP203) to interpret the product model data represented by the STEP AP203 format, and realize the recognition of B spline surface features. Hussein *et al.* [11] constructed the corresponding function module according to the STEP AP203 format of automobile exterior contour, and realized the recognition and extraction of 11 different kinds of features. Sunil and Pande [12] designed and implemented the feature recognition method for the part surfaces of STL format sheet metal. And a segmentation algorithm based on edge region mixing is proposed, the pretreated STL model is divided into meaningful regions for recognition and classification by the geometric properties on model. Kataraki and Abu Mansor [13] proposed a rule-based method for SAT format files to identify fillet features on parts that represented by B-Rep. Benhabiles *et al.* [14] proposed a fully automatic mesh segmentation algorithm, using Ada Boost algorithm to train the classifier and using active contour model to obtain smooth segmentation results. Theologou *et al.* [15] presented a fully automatic mesh segmentation scheme using heterogeneous graphs. They developed an unsupervised spectral framework in which local geometry affinities are coupled with surface patch affinities; the segmentation results were comparable to those of best supervised approaches. Muraleedharan *et al.* [16] presents a method to identify regions that make up features like holes, slots, pockets as well as interacting features in a three-dimensional mesh of a CAD model. Clustering-based decomposition or extraction of feature lines by solid or curvature values are used in most feature recognition methods. The proposed algorithm identifies the features using contours generated by random cutting planes, followed by graph traversals and without using threshold values. The algorithm can identify blind holes, through holes, slots and pockets. The geometry of most of the extracted features has also been identified using Gauss map. Tao Pin *et al.* [17] designed a method to decompose the model into several parts with the hints from bottom faces, concave vertexes and concave edges, etc. And also a coding algorithm based on the face relation matrix (FRM) was given to translate the topology data of a part into the vector, which can be proceeded by the neural networks. Katz *et al.* [18] proposes a novel hierarchical mesh segmentation algorithm, which is based on new methods for prominent feature point and core extraction. First, it is invariant both to the pose of the model and to different proportions
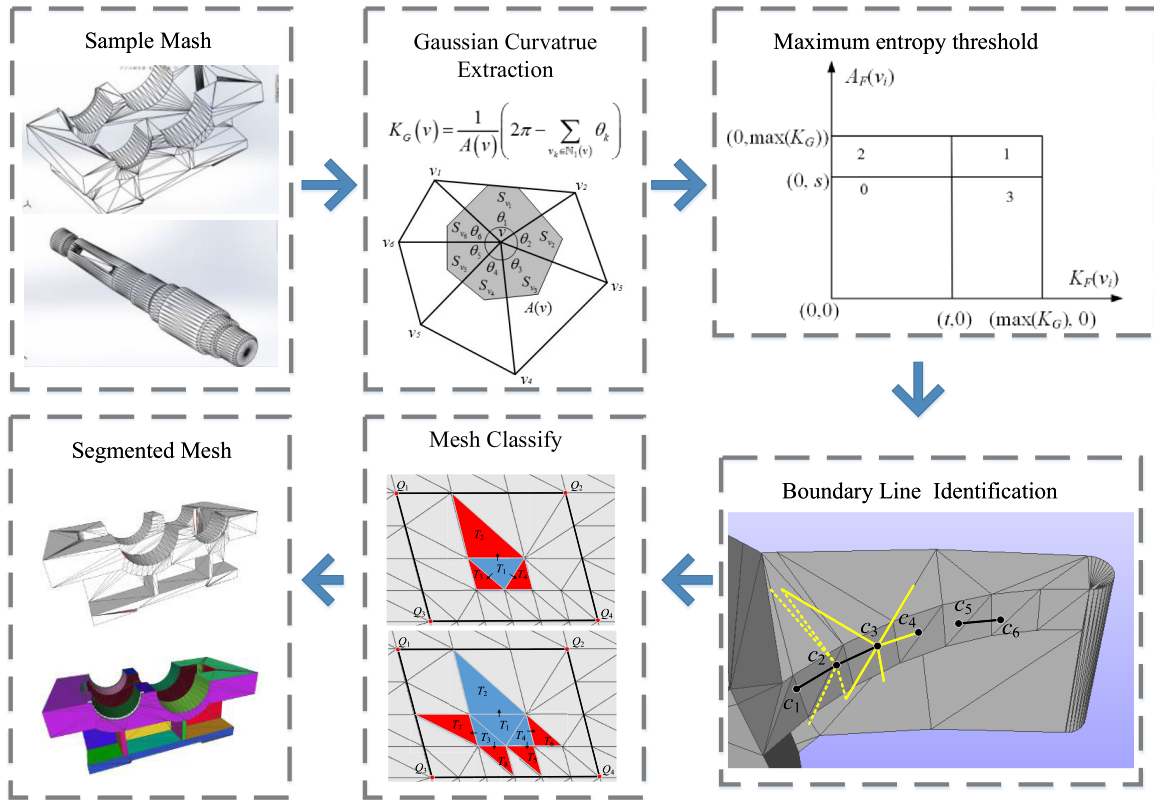
FIGURE 1. An overview of our surface division method.

between the model's components. Second, it produces correct hierarchical segmentations of meshes, both in the coarse levels of the hierarchy and in the fine levels, where tiny segments are extracted. Finally, the boundaries between the segments go along the natural seams of the models. Hoffman *et al.* [19] proposed a theory on human visual perception object recognition, in which a rule called minimum rule was introduced for dividing surfaces into parts. The minimum rule suggests dividing an object into parts of each negative minimum point of the principal curvature according to the transverse principle: forming a concave crease at the intersection of two three-dimensional shapes. Au *et al.* [20] proposed a framework extraction method based on mesh shrinkage to contract the mesh to skeleton shape by implicit Laplacian smoothing with global position constraints and provide a regional reference for mesh segmentation. Zhang *et al.* [21] used spectral clustering-based mesh segmentation as segmentation initialization method to construct a new Laplace matrix, which can reflect more semantic information than classical Laplace matrix and provide good initial segmentation results for subsequent accurate segmentation. Wu *et al.* [22] improved the traditional spectral clustering method to construct a similarity matrix of shape descriptors, use it to generate good segmentation results by performing spectral clustering in the fusion space of shape descriptors.

Overall, the research results mentioned above provide some effective methods for mesh model of non-mechanical parts. However, unlike the usual model mesh division,

the actual mechanical parts have clear geometric boundaries. The mesh division process is actually to accurately search the existing boundaries, while the usual mesh model does not have clear boundaries to generate eligible boundary according to specific requirements. On the other hand, some existing algorithms are related to machine learning, and there is a defect that the training time is too long to adapt to the efficient mechanical production environment.

III. OVERVIEW

In this paper, a surface partition method of part grid model with Gaussian curvature, hierarchical clustering and region growth is proposed. First we calculated the Gaussian curvature of all coordinate points in the grid model. Second we use hierarchical clustering to calculate the curvature threshold of boundary points, then the boundary line is constructed for the extracted boundary points, and the angle between the three corners of the boundary line is calculated. After that we calculated the angle threshold of boundary by the maximum entropy threshold method, the extracted boundary is then closed tested. At last, the triangular slices in each boundary are classified by region growth algorithm, and the mesh model surface partition is completed. Overall process is shown in Fig 1.

1) Temporary boundary point extraction for part mesh model. The first step of this method is to extract all the coordinate points that can form the boundary on the mesh model of part, so we need to calculate the

curvature value of each coordinate point. According to the Gauss-Bonnet method, the Gaussian curvature at any discrete coordinate points on the mesh model can be estimated [23]. By using the two-dimensional maximum entropy threshold method, these curvature can be aggregated into two data sets with obvious differences, in which the temporary boundary points within the set with larger curvature can be constructed as boundary lines.

2) Construction and extraction of boundary lines. According to the temporary boundary points, each temporary boundary line is the common edge of two triangular mesh. All these angle distribution relations can be obtained by calculating the angle between two triangular mesh. The maximum between-class variance method is used to divide the angle value into two categories, so the boundary line on the part mesh model can be extracted from the temporary boundary line.

3) Close test of the boundary line. Sometimes the extracted boundary line is unclosed, so the boundary line needs a close test. According to the characteristic of loop that often exists on the part boundary, and refer to the concept of ant colony algorithm, the search situation of each boundary is recorded by constructing a boundary loop matrix. For the boundary vector in the matrix, if the loop cannot be formed during searching, it is necessary to implement the broad priority traverse from breakpoint to find the corresponding breakpoint and complete the patch of unclosed boundary.

4) Acquisition of the triangle mesh within the boundary. When the boundary search is completed, we begin to classify triangular mesh within each boundary. The triangular mesh is randomly selected from the part mesh model and continuously expanded according to the region growth algorithm. In this process, we judge whether the newly added triangular mesh reaches the boundary, and then traverse all the triangular mesh on the part to complete the classification of surface mesh.

IV. BOUNDARY LINE EXTRACTION OF PART MESH MODEL BASED ON HIERARCHICAL CLUSTERING

A. ESTIMATION OF GAUSSIAN CURVATURE IN COORDINATE POINTS

The curvature is the key parameter to reflect the bending degree of geometric surface. According to the related concept of differential geometry, for a point P on surface S, we call the two eigenvalues k_1 and k_2 of Weingarten transform on P point as the main curvature of surface S at P point, then we have the curvature $K = k_1 k_2$. According to the analysis of Princeton Segmentation Benchmark (PSB) mesh model, the curvature of the model boundary is often larger than the non-boundary region [24]. Therefore, it is important to consider the Gaussian curvature value of coordinate points in the process of extracting boundary points, which can be used as a reference for dividing boundary and non-boundary.

When a part mesh model is acquired, the boundary point curvature threshold is defined as K_{TH}, if the coordinate point curvature is greater than the threshold, the point is extracted as a boundary candidate.
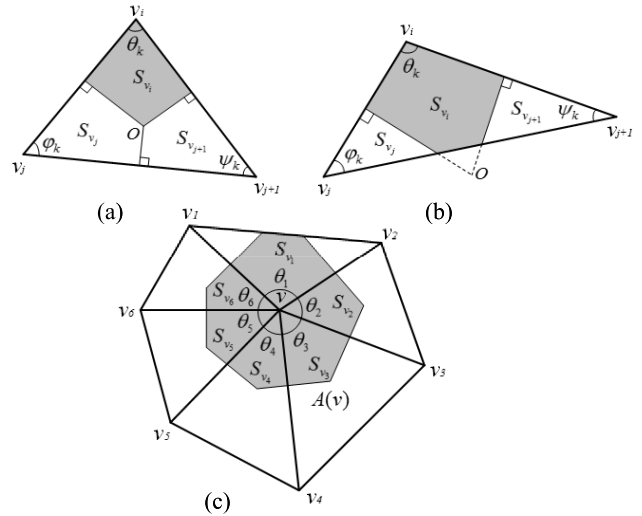

FIGURE 2. Schematic diagram of vertex Gaussian curvature threshold estimation in triangular mesh model.

The vertex Gaussian curvature estimation of the triangular mesh model includes the position relation of the triangular plane slice in its first order neighborhood, that is, the vertex and its one-dimensional neighborhood vertex coordinates. As shown in Fig.2, we define v_i, v_j and v_{j+1} as the vertex of triangle mesh T, and define the angle between edge $v_i v_j$ and $v_j v_{j+1}$ as φ_i, define the angle between edge $v_i v_{j+1}$ and $v_j v_{j+1}$ as Ψ_i. By the Gauss–Bonnet formula we can infer that

$$K_G(v_i) = \frac{1}{A(v_i)} \left(2\pi - \sum_{v_k \in \mathbb{N}_1(v)} \theta_k \right) \quad (1)$$

where $K_G(v_i)$ represents the Gaussian curvature of vertex v_i, $A(v_i)$ represents the region area that neighborhood triangle mesh of vertex v_i corresponding to, θ_k represents the angle between vertex v_i and k-th triangle mesh of vertex v_i neighborhood. $A(v_i)$ can be represent as follow

$$A(v) = \sum_i S_{v_i} \quad (2)$$

where S_{vi} represents the Voronoi diagram area (which are marked in gray in Fig.2) vertex v_i neighborhood, the value of S_{vi} based on rule as follow [25]

$$S_{v_i} = \begin{cases} \frac{1}{8} \left(\|v_i v_{j+1}\|^2 \cot \varphi_k + \|v_i v_j\|^2 \cot \psi_k \right), & 0 < \theta_k \leq \frac{\pi}{2} \\ \frac{1}{2} \|v_i v_j\| \|v_i v_{j+1}\| \sin \theta_k \\ -\frac{1}{8} \left(\|v_i v_j\|^2 \tan \varphi_k + \|v_i v_{j+1}\|^2 \tan \psi_k \right), & \frac{\pi}{2} < \theta_k < \pi \end{cases}$$

$$(3)$$

As shown in Fig.2(c), we use vertex v as example, the Gaussian curvature of this vertex can be estimate as follow

$$K_G(v) = \frac{2\pi - \sum\limits_{v_k \in \mathbb{N}_1(v)} \theta_k}{A(v)}$$

$$= \frac{2\pi - (\theta_1 + \theta_2 + \theta_3 + \theta_4 + \theta_5 + \theta_6)}{S_{v_1} + S_{v_2} + S_{v_3} + S_{v_4} + S_{v_5} + S_{v_6}} \quad (4)$$

B. CURVATURE THRESHOLD ANALYSIS BASED ON TWO-DIMENSIONAL MAXIMUM ENTROPY THRESHOLD SEGMENTATION

There are a large number of coordinate points on part mesh model, and only some of them are located on the boundary of part, so it is necessary to analyze the Gaussian curvature of each vertex and extract the coordinate points belonging to the boundary. It can be seen from the above that the Gaussian curvature of all coordinate points are one-dimensional data, then we use the two-dimensional maximum entropy threshold segmentation to divide the curvature data into two categories, which contains the coordinate points that can form the boundary and cannot form the boundary.

During the segmentation of part mesh model, it needs a threshold to divide the curvature data. We defined m as the quantity of coordinate points on model, set $G_S = \{K_G(v_1), K_G(v_2), \ldots, K_G(v_m)\}$ included the curvature value of all coordinate points, $\max(K_G)$ and $\min(K_G)$ represents the maximum curvature and minimum curvature. For making the subsequent calculation easier, we divided the G_S into several interval, and set parameter int as the quantity of interval, parameter stp as the step, then we have

$$stp = \frac{\max(K_G) - \min(K_G)}{int} \quad (5)$$

so the curvature grade can be classified as $F = [\min(K_G), \min(K_G) + stp, \ldots, \min(K_G) + (int-1)stp, \max(K_G)]$. Taking the neighborhood average curvature grade $A_G(v_i)$ as curvature $K_G(v_i)$, and we have

$$A_G(v_i) = \frac{1}{d} \sum_{k \in D} F[k] \quad (6)$$

where D represents the point set, elements within it are all adjoin the current coordinate point, d represents the quantity of coordinate points in D. We defined $K_F(v_i)$ as the corresponding curvature grade of $K_G(v_i)$ in F, $A_F(v_i)$ as the corresponding curvature grade of $A_G(v_i)$ in F, $r(i,j)$ represents the frequency of $[K_F(v_i), A_F(v_i)]$ and define the two-dimensional histogram $p(i,j) = r(i,j)/m$ as shown in Fig.3

Assume the probability of non-boundary curvature and boundary curvature are $\omega_0(t,s)$ and $\omega_1(t,s)$, shown as follows

$$\begin{cases} \omega_0(t,s) = \sum\limits_{i=0}^{t} \sum\limits_{j=0}^{s} p(i,j) \\ \omega_1 \approx 1 - \omega_0(t,s) \end{cases} \quad (7)$$

mean value of curvature grade are $\mu_{0i}(t,s)/\omega_0(t,s)$, $\mu_{0j}(t,s)/\omega_0(t,s)$, $\mu_{1i}(t,s)/\omega_1(t,s)$, $\mu_{1j}(t,s)/\omega_1(t,s)$,
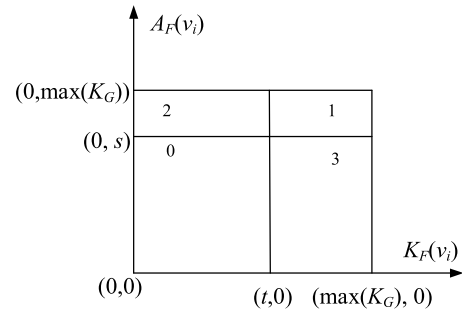

FIGURE 3. The two-dimensional histogram of curvature.

shown as follows

$$\begin{cases} \mu_{0i}(t,s)/\omega_0(t,s), \mu_{0i}(t,s) = \sum\limits_{i=0}^{t} \sum\limits_{j=0}^{s} ip(i,j) \\ \mu_{0j}(t,s)/\omega_0(t,s), \mu_{0j}(t,s) = \sum\limits_{i=0}^{t} \sum\limits_{j=0}^{s} jp(i,j) \\ \mu_{1i}(t,s)/\omega_1(t,s), \mu_{1i}(t,s) = \sum\limits_{i=t+1}^{\max(K_G)} \sum\limits_{j=s+1}^{\max(K_G)} ip(i,j) \\ \mu_{1j}(t,s)/\omega_1(t,s), \mu_{1j}(t,s) = \sum\limits_{i=t+1}^{\max(K_G)} \sum\limits_{j=s+1}^{\max(K_G)} jp(i,j) \end{cases} \quad (8)$$

variance $\sigma_{0i}^2(t,s), \sigma_{0j}^2(t,s), \sigma_{1i}^2(t,s), \sigma_{1j}^2(t,s)$ are shown as follows

$$\begin{cases} \sigma_{0i}^2(t,s) = \sum\limits_{i=0}^{t} \sum\limits_{j=0}^{s} [i - \mu_{0i}/\omega_0(t,s)]^2 \cdot p(i,j)/\omega_0(t,s) \\ \sigma_{0j}^2(t,s) = \sum\limits_{i=0}^{t} \sum\limits_{j=0}^{s} [j - \mu_{0j}/\omega_0(t,s)]^2 \cdot p(i,j)/\omega_0(t,s) \\ \sigma_{1i}^2(t,s) = \sum\limits_{i=t+1}^{\max(K_G)} \sum\limits_{j=s+1}^{\max(K_G)} [i - \mu_{1i}/\omega_1(t,s)]^2 \\ \cdot p(i,j)/\omega_1(t,s) \\ \sigma_{1j}^2(t,s) = \sum\limits_{i=t+1}^{\max(K_G)} \sum\limits_{j=s+1}^{\max(K_G)} [j - \mu_{1j}/\omega_1(t,s)]^2 \\ \cdot p(i,j)/\omega_1(t,s) \end{cases} \quad (9)$$

then we have the selection criterion function of 2D vertical segmentation threshold based on intra-class variance and area deviation between boundary curvature and non-boundary curvature

$$\Phi(t,s) = \frac{[\omega_0(t,s) - \omega_1(t,s)]^2}{\omega_0(t,s)\left[\sigma_{0i}^2(t,s) + \sigma_{0j}^2(t,s)\right] + \omega_1(t,s)\left[\sigma_{1i}^2(t,s) + \sigma_{1j}^2(t,s)\right]} \quad (10)$$

To maximize the value of the criterion function, the curvature grade $K_F(v_i)$ corresponding to the parameter (t,s) is the

obtained curvature partition threshold. The boundary point set C_B and the non-boundary point set obtained according to the threshold C_{NB} will be taken as the preliminary extraction result of the boundary from part model and further refined in the subsequent analysis.

C. MODEL BOUNDARY LINE EXTRACTION AND OPTIMIZATION

Some coordinate points that cannot construct the boundary line may exist in boundary point set C_B, which needs to be extracted. For the triangular mesh model of any part, if there is a straight line connection between the two coordinate points, then the two coordinate points must be located on the same triangle. The data format of the mesh model contains three vertices of each triangular mesh, so it is easy to obtain all the coordinate points connected with a particular point on the model, and we constructed the adjacency matrix M_{AD} of the boundary point set C_B, as follows

$$M_{AD} = \begin{bmatrix} a_{11} & a_{12} & \cdots & a_{1n} \\ a_{21} & a_{22} & & a_{2n} \\ \vdots & & \ddots & \vdots \\ a_{n1} & a_{n2} & \cdots & a_{nn} \end{bmatrix} \quad (11)$$

where n represents the element quantity in point set C_B, a_{ij} represents the adjacency relation between i-th coordinate point and j-th coordinate. Taking $a_{ij} = 1$ represents there is adjacency relation between two coordinate points (which means the two coordinate points can be linked by a straight line), $a_{ij} = 0$ represents there is no adjacency relation between two coordinate points, and we defined each coordinate point is not adjacent to itself, which is $[a_{11}, a_{22}, \ldots, a_{nn}]=0$.

1) MODEL BOUNDARY LINE EXTRACTION BASED ON MAXIMUM BETWEEN-CLUSTER VARIANCE

According to the adjacency matrix M_{AD}, all lines between points can be extracted from the point set C_B. For any two coordinate points Q_a and Q_b in C_B with adjacency relation, assume a set L_S represents the straight line connecting them, then we have $L_S=\{Q_a, Q_b\}$. Let L_A be a set of all lines in C_B, then there are $L_A = \{L_{S1}, L_{S2}, \ldots, L_{Sn}\}$. According to the STL format data of mesh model, it can be quickly found out any two triangle a and b within L_A that share a same line, meanwhile the vector v_a and v_b of the triangles can be obtained, so the angle θ_{ab} between two triangles is as follow

$$\cos\theta_{ab} = \cos\langle v_a, v_b\rangle = \frac{v_a \cdot v_b}{|v_a| \cdot |v_b|} \quad (12)$$

On the basis of adjacency matrix M_{AD}, the angle matrix M_θ of vector can be constructed, it is about the angle of the triangles that share a same edge (co-edge triangle). According to those elements in M_{AD} with its value equals 1, it can be quickly calculated all angles of co-edge triangle. For those elements in M_{AD} with value 0, the value of their angle θ is -1,

as shown in formula 13

$$M_\theta = \begin{bmatrix} \theta_{11} & \theta_{12} & \cdots & \theta_{1n} \\ \theta_{21} & \theta_{22} & & \theta_{2n} \\ \vdots & & \ddots & \vdots \\ \theta_{n1} & \theta_{n2} & \cdots & \theta_{nn} \end{bmatrix} \quad (13)$$

where n represents the quantity of elements in line set L_A, θ_{ij} represents the angle of the triangular mesh which simultaneously contains the i-th and j-th coordinates. When extracting the boundary line, it needs to be distinguished by the angle threshold, in this paper, the Maximum Between-cluster Variance [26] is used to analyze the angle threshold. We defined m as the quantity of elements that angle value between vectors is not equals -1, set θ_S represents the non-negative angle value in the matrix M_θ, $\max(\theta_S)$ and $\min(\theta_S)$ represent the maximum angle and the minimum angle in the θ_S. To facilitate the subsequent calculation, we divided the angle in θ_S into several intervals, and the step size of the angle division is stp, so we have

$$stp = \frac{\max(\theta_S) - \min(\theta_S)}{m} \quad (14)$$

the angle grade of M_θ can be classified as $[\min(\theta_S), \min(\theta_S)+stp, \ldots, \min(\theta_S) + (m-1)stp, \max(\theta_S)]$. We defined L_θ as the threshold of angles, for extracting the boundary line on mesh model, we created set θ_{NB} and set θ_B to represent non-boundary angle set and boundary angle set. The probability for each set is as follows

$$\begin{cases} w_0 = P(\theta_{NB}) = \sum_{j=1}^{i} p_j = w(L_\theta) \\ w_1 = P(\theta_B) = \sum_{j=i+1}^{m} p_j = 1 - w(L_\theta) \end{cases} \quad (15)$$

where p_j represents the probability of j-th angle. The average angel of each interval is

$$\begin{cases} u_0 = \sum_{j=1}^{i} j \times P(j|\theta_{NB}) \\ u_1 = \sum_{j=i+1}^{m} j \times P(j|\theta_B) \end{cases} \quad (16)$$

so the between-cluster variance, intra-class variance and total variance are shown as follows

$$\begin{cases} u_T = \sum_{j=1}^{m} j \times p_j \\ \delta_B^2(L_\theta) = w_0(u_0 - u_T)^2 + w_1(u_1 - u_T)^2 \\ \delta_W^2(L_\theta) = w_0 \sum_{j=1}^{i}(j - u_0)^2 P(j|\theta_{NB}) \\ \quad + \sum_{j=i+1}^{m}(j - u_1)^2 P(j|\theta_B) \\ \delta_T^2 = \delta_B^2(L_\theta) + \delta_W^2(L_\theta) = const \end{cases} \quad (17)$$
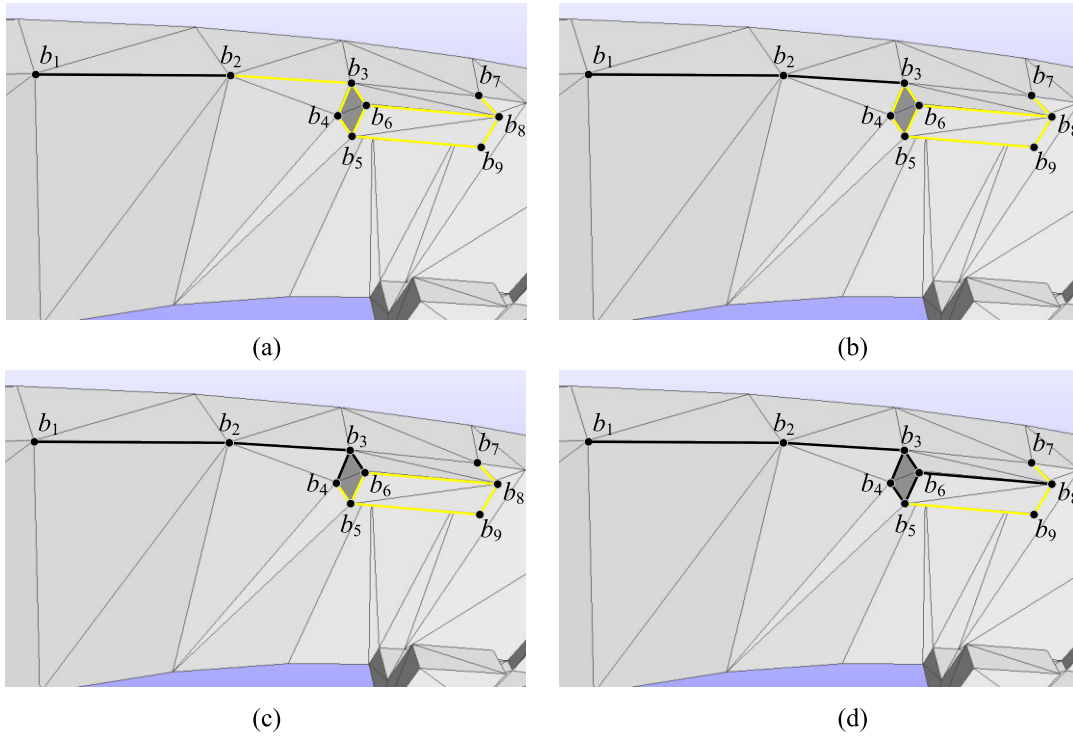
(a)　　　　　　　　　　(b)

(c)　　　　　　　　　　(d)

FIGURE 4. Schematic diagram of vertex Gaussian curvature threshold estimation in triangular mesh model.

Because the total variance is constant, choosing the appropriate L_θ makes $\delta_B^2(L_\theta)$ to the maximum, at this time, the threshold L_θ of the maximum inter-class variance is the standard for extracting the boundary line, the boundary line is the common edge of the triangle surface.

2) BOUNDARY CLOSE TEST

The boundary extracted according to the above method may have the condition that boundary is not closed, so it is necessary to do the boundary close test. The eligible coordinate pairs in M_θ are extracted according to the angle threshold L_θ to form a set of boundary lines as $L_b = \{(b_i, b_j) \,|\, b_i, b_j \in b\}$. The b_i and b_j represent the endpoint coordinates of a straight line, b represents the set of all coordinate points that meet the conditions. Some of these boundaries do not have branches on the endpoint for the set L_b, and for this class of boundary elements it can be merged into a branchless element, as shown in Fig 4. All points in the figure are boundary points, and the inspection process is as follows

Step 1 Select the starting boundary: As shown in Fig.4(a)(b), we selected line b_1b_2 as starting boundary, the boundaries that contain the coordinate point b_2 are b_1b_2 and b_2b_3, from this we know that line b_1b_2 only extends to b_2b_3 without branch, so line b_1b_2 and line b_2b_3 can be combined to line b_1b_3, it helps to reduce data size, at this moment the boundary b_1b_3 included three coordinate points (b_1, b_2, b_3), b_1 and b_3 are the index for subsequent test.

Step 2 Process the boundary branch: Generally, a small segment of boundary on the part surface is in a boundary loop,

many of which together form the geometric boundary of part. In this process, the same segment boundary may be shared by multiple loops, so it cannot be used as a condition when judging the boundary closure, it needs to be analyzed for the minimized loop. As shown in Fig.4(c), a branch appears on boundary b_1b_3 at point b_3, line b_3b_4 and b_3b_6 are all boundaries. We defined the boundary matrix B_M for part mesh model, as shown in Fig.5, the initial boundary vector B_{M1} includes one boundary formed by three coordinate points, when a branch generated at b_3, two new boundaries b_3b_4 and b_3b_6 that begin with b_3 become new boundary vectors (the empty parts fulfilled by 0), meanwhile B_{M1} extends itself to b_4 and b_6, the matrix updated to B_{M2}, each row in B_{M2} represents a boundary.

Step 3 Process of duplicate paths: After each boundary in the matrix B_{M2} continues to extend, the matrix is updated to B_{M3}, it can be seen that there are two pairs of identical boundary vectors in the updated matrix, as shown in Fig 5. The first value of 0 indicates that the vector is derived from branch point splitting, such as $[0, 0, 0, b_6, b_8]$ indicates the boundary that starting point is b_6 and is currently tested to b_8. For all the boundary vectors with first element value is 0, when the first and second non-zero elements are equal, the boundary vectors have equal relations, that is, representing the same boundary, and the repeated vectors can be deleted at this time.

Step 4 Boundary loop close judgment: Following the steps above to traverse the boundary set L_b and update the boundary matrix B_M, as B_{M3} and B_{M4} in Fig 5. When the newly added boundary point of any current boundary vector is the same
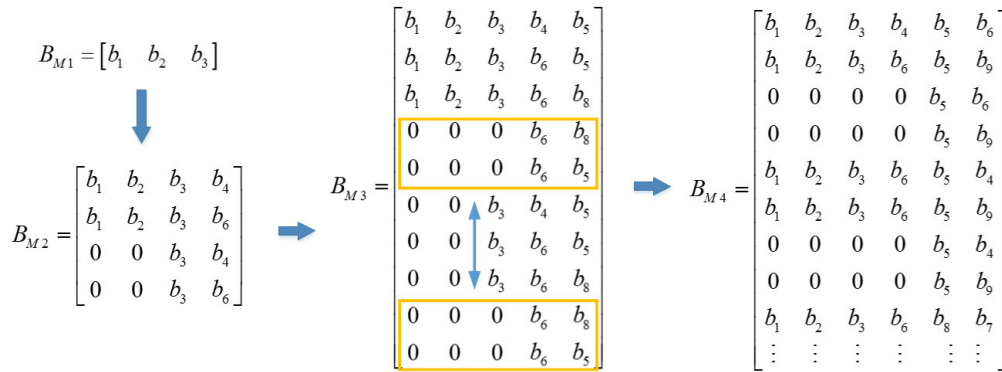
$$B_{M1} = \begin{bmatrix} b_1 & b_2 & b_3 \end{bmatrix}$$

$$B_{M2} = \begin{bmatrix} b_1 & b_2 & b_3 & b_4 \\ b_1 & b_2 & b_3 & b_6 \\ 0 & 0 & b_3 & b_4 \\ 0 & 0 & b_3 & b_6 \end{bmatrix}$$

$$B_{M3} = \begin{bmatrix} b_1 & b_2 & b_3 & b_4 & b_5 \\ b_1 & b_2 & b_3 & b_6 & b_5 \\ b_1 & b_2 & b_3 & b_6 & b_8 \\ 0 & 0 & 0 & b_6 & b_8 \\ 0 & 0 & 0 & b_6 & b_5 \\ 0 & 0 & b_3 & b_4 & b_5 \\ 0 & 0 & b_3 & b_6 & b_5 \\ 0 & 0 & b_3 & b_6 & b_8 \\ 0 & 0 & 0 & b_6 & b_8 \\ 0 & 0 & 0 & b_6 & b_5 \end{bmatrix}$$

$$B_{M4} = \begin{bmatrix} b_1 & b_2 & b_3 & b_4 & b_5 & b_6 \\ b_1 & b_2 & b_3 & b_6 & b_5 & b_9 \\ 0 & 0 & 0 & 0 & b_5 & b_6 \\ 0 & 0 & 0 & 0 & b_5 & b_9 \\ b_1 & b_2 & b_3 & b_6 & b_5 & b_4 \\ b_1 & b_2 & b_3 & b_6 & b_5 & b_9 \\ 0 & 0 & 0 & 0 & b_5 & b_4 \\ 0 & 0 & 0 & 0 & b_5 & b_9 \\ b_1 & b_2 & b_3 & b_6 & b_8 & b_7 \\ \vdots & \vdots & \vdots & \vdots & \vdots & \vdots \end{bmatrix}$$

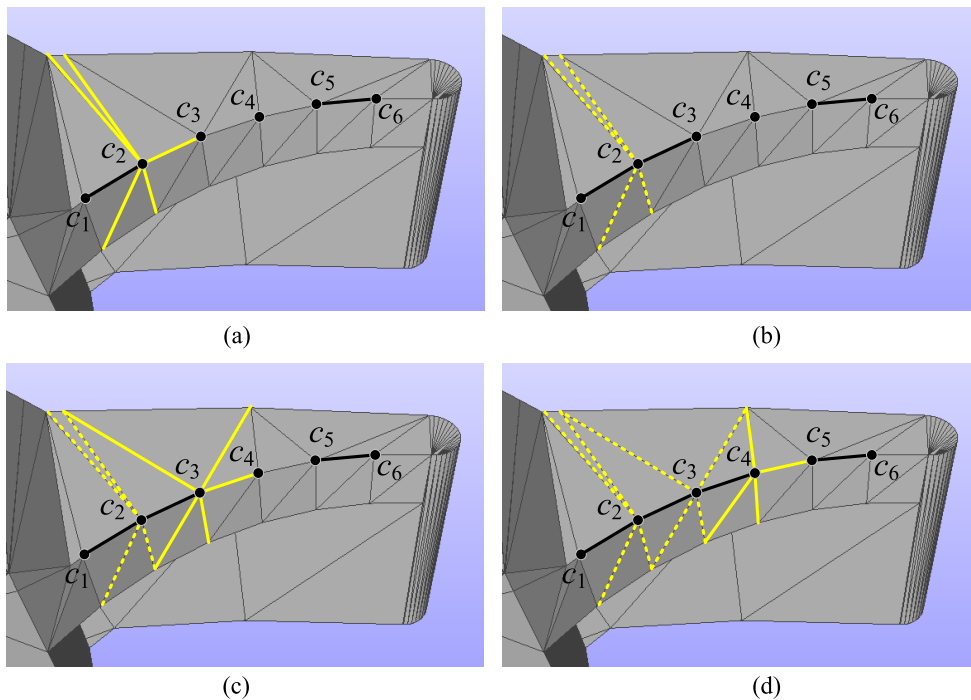**FIGURE 5.** Boundary matrix B_M for part mesh model.

FIGURE 6. Part mesh model boundary breakpoint search process. The yellow line represents the edge we currently searching, the yellow dotted line represents the edge we searched, and the black line represents the new boundary that newly added.

as its initial boundary point, it indicates that the boundary has formed a closed loop. In the subsequent update of the boundary matrix, the boundary vector can only be supplemented with 0. Assume that the matrix dimension is $m \times n$ after updating, if the n-th column elements value are all 0, then all the boundaries are traversed and no new boundaries are added.

In the above test, there may have some boundary breakpoints, which means a boundary missing in the place where there should be a boundary, so it needs to be searched out from the breakpoint along the edge of the adjacent triangular plane until the connection with the known boundary is established. The search at the breakpoint is actually a screening of all possible boundaries, which is gradually extended by analyzing the similarity between the breakpoint and the angle of triangle mesh on each boundary connected with the breakpoint, until the connection with the known boundary is established. Specific steps are as follows

Step 1 Correlation boundary selection: As shown in Fig.6(a), taking point c_2 as the breakpoint, the searching starts from boundary $c_1 c_2$, the other breakpoint is c_5. According to part mesh model data we can acquire the coordinate point set V_{c2} that all points adjacent to c_2, and its corresponding edge (those yellow lines in Fig.5a) set is E_{c2}, each edge in E_{c2} is shared by two adjacent triangle mesh, then we can get a vector pair (v_i, v_j) to represents the two adjacent triangle
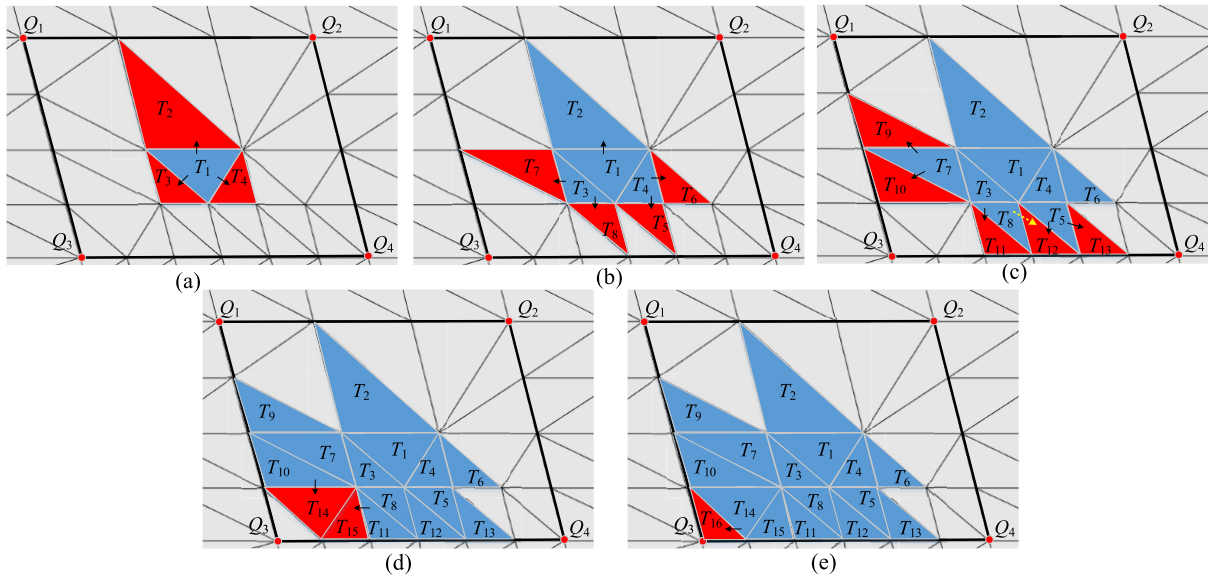
FIGURE 7. Classification of triangle mesh in part mesh model.

mesh and calculate its angle $\theta_{ij} < v_i, v_j >$. Assume that vector pair angle of boundary c_1c_2 is θ_{12} and create a vector pair angle set θ_{c2} for all vectors in E_{c2}, then the element that most similar to θ_{12} in θ_{c2} is the next point which current breakpoint extend to, as the newly added edge c_2c_3 shown in Fig.6(b). Meanwhile the breakpoint transfer to c_3 and next search start from new breakpoint c_3.

Step 2 Boundary breakpoint update: Repeat the *Step 1* to gradually search out the missing boundary, as shown in Fig. 6(c), while updating the boundary matrix and boundary vector where the breakpoint is located.

Step 3 Boundary search endpoint judgment: As shown in Fig 6(d), as the search process continues, the set V_{c4} that all coordinate point adjacent to the current breakpoint c_4 contains the known breakpoint c_5, indicating that the current incomplete boundary has been completed and the new boundary vector added to boundary matrix B_M is (c_2, c_3, c_4, c_5).

V. CLASSIFICATION OF TRIANGLE MESH WITHIN BOUNDARY BASED ON REGION GROWTH ALGORITHM

The boundary of part mesh model can be obtained by the method mentioned above, then according to the boundary we classified the triangle mesh on the model surface into the region it belongs to complete the segmentation of mesh model surface. The triangle mesh on mesh model only contains adjacent relations, so during division process we refer to region growth algorithm, by selecting the initial triangle mesh as the seed to gradually pick out all the mesh within current boundary. The steps are as follows:

Step 1 Initial seed mesh selection: As shown in Fig.7(a), select a triangle mesh T_1 on part model randomly. Assume that the boundary of T_1 is (Q_1, Q_2, Q_3, Q_4), set Q_S includes all points on boundary, set T_{Qs} includes all mesh within

boundary and its initial status is empty, the vertex on k-th triangle mesh T_k stored in set Q_{Tk}. For triangle mesh T_1, if the selected triangle mesh shares an edge with it, then this triangle mesh can be added to Q_{Tk}, the rule is as follow

$$|Q_{T1} \cap Q_{Tk}| = 2 \qquad (18)$$

Step 2 Position determination of triangle mesh: For a triangle mesh in the direction of growth, it is necessary to judge whether the triangle mesh is located within the boundary Q_S. Fig 7(c) shows that a vertex on mesh T_7 is coincide with boundary points, but it can still extend to mesh T_9 and T_{10}. For mesh T_{10}, it has two vertexes in set Q_S, so it cannot extend in the direction formed by these two points. On the other hand, as shown in Fig 7(e), though T_{14} has two vertexes coincide with boundary points, it can still extend to the mesh T_{16} in the corner, at this time, all vertexes on T_{16} are coincide with boundary. Assume that triangle mesh T_c is the current mesh in Q_S, for any adjacent triangle mesh T_k, if it satisfied the following rules then T_k should not add to Q_{Tk}.

$$(((Q_{Tc} \cap Q_{Tk}) \neq (Q_{Tc} \cap Q_S)) \wedge (|Q_{Tc} \cap Q_{Tk}| = 2)) \\ \vee (|Q_{Tc} \cap Q_S| = 3) \qquad (19)$$

Step 2 Process for repeated triangle mesh: Repeat the above steps to finish triangle mesh classification, some of the mesh may be added repeatedly during the process, as T_{12} in Fig.7(c), it can be retrieved by T_5 and T_8. To prevent repeated additions, make the following judgment whenever a new triangle is added during growth

$$\begin{cases} (Q_{Tk} - (T_{Qs} \cap Q_{Tk})) = \emptyset \rightarrow Q_{Tk} \subseteq T_{Qs} \\ (Q_{Tk} - (T_{Qs} \cap Q_{Tk})) \neq \emptyset \rightarrow Q_{Tk} \not\subset T_{Qs} \end{cases} \qquad (20)$$

if the coordinate point in Q_{Tk} that doesn't belong to T_{Qs}, it means Q_{Tk} can be added into T_{Qs} as a new triangle mesh,
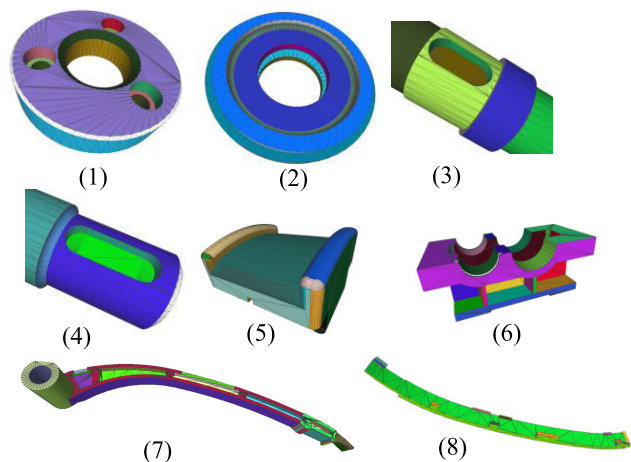
FIGURE 8. Segmentation results of part mesh model using our method.

otherwise it means that Q_{Tk} has been retrieved and will not be added into T_{Qs}.

VI. EXPERIMENTAL TESTS AND RESULTS ANALYSIS

To verify the effectiveness of the method, the verification model selected in this paper comes from the actual production process in mechanical field, some of which contain obvious boundaries, others contain non-obvious boundaries such as rounded corners, transition edges, etc. As shown in Fig.8, the number of triangular slices contained in each instance

TABLE 1. Comparison of processing time with reference 27.

Model Number	1	2	3	4	5	6	7	8
Ours	7.8	9.2	9.0	6.1	9.2	6.8	11.0	9.0
Ref. 27	14.1	16.3	13.5	8.9	14.0	8.6	20.3	9.2

varies from thousands to tens of thousands. In order to make the final partition more obvious, the area is marked with different colors.

Reference [27] also processed the model by extracting the boundary, so it is used to compare with the method in this paper, the segmentation results of the model are shown in Fig.9, in order to reflect the final partition results, the surface of mesh model in the figure is labeled with different colors in different regions. In contrast, the method in this paper has a better effect on the segmentation results. As shown in the figure, in some parts of the model where the boundaries are more compact, this method obtains more realistic segmentation results, similarly, in some transition regions, the boundary separated by this method is smoother. It can be seen from the figure, the results of Ref.27 cannot accurately divide the regions in some locations where some edges and interferences close to each other. For some corners with surface features, Ref. 27 does not delineate them well, and the method in this paper does. The comparison of processing time is shown in Table.1.
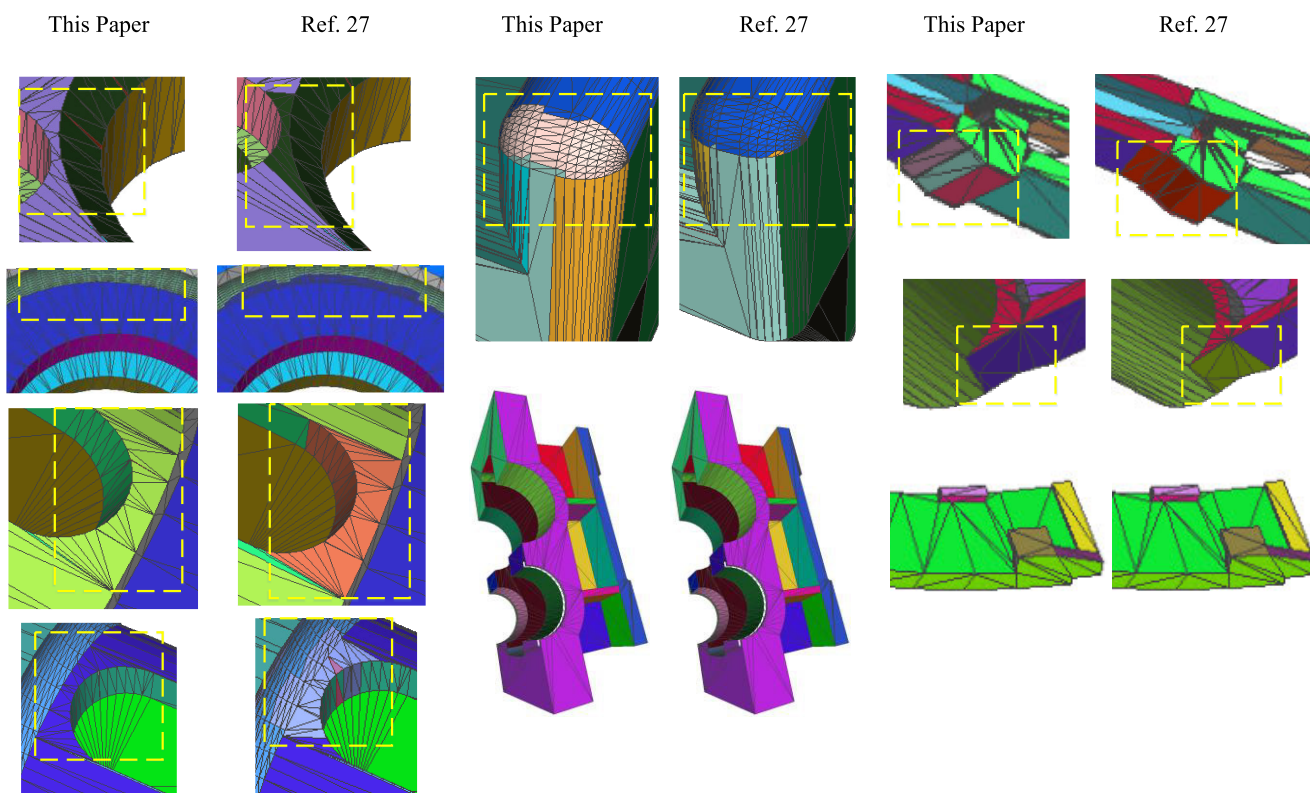

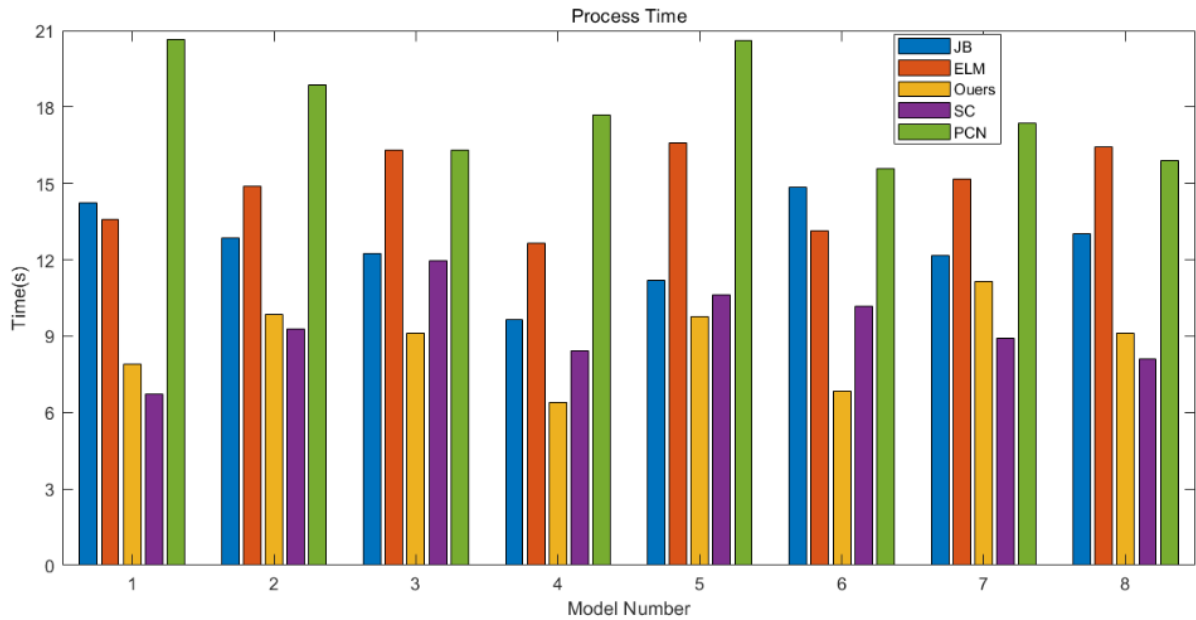**FIGURE 9.** Segmentation results of part mesh model using our method.

FIGURE 10. Comparison of processing time using 5 algorithms.

TABLE 2. Processing time statistics using 5 algorithms.

Model Number	JointBoost	Projective Convolutional Network	ELM	Spectral Clustering	This Paper
1	14.2	20.9	13.9	6.9	7.8
2	13.1	18.3	14.9	9.0	9.2
3	12.5	16.8	16.5	11.9	9.0
4	10.3	17.6	12.2	8.5	6.1
5	11.8	20.8	16.4	10.5	9.2
6	15.0	15.2	13.2	10.0	6.8
7	12.1	17.8	15.0	9.0	11.0
8	12.9	16.0	16.5	8.1	9.0

Most of the current mesh segmentation methods involve machine learning theory, which aims to obtain satisfactory segmentation results by using existing intelligent algorithms to train a large number of models, which contains two mainstream ways: supervised training and unsupervised training. Therefore, this paper combines four commonly used machine learning models for test comparison, including three supervised learning algorithms: ELM [28], JointBoost (JB) [29], Projective Convolutional Networks (PCN) [30] and an unsupervised learning algorithm Spectral Clustering (SC) [31]. The operation processing time of each algorithm is shown in Fig.10, it can be seen that our method has advantages in processing time, and the average processing time is low. The computation time of five algorithms in the process of processing part mesh model is shown in Table.2. The average time used in each method in model segmentation is: 12.73s (JointBoost), 17.92s (Project Convolutional Network), 14.82s (ELM), 9.24s (Spectral Clustering) and 8.51s (This Paper). Obviously, compared with other machine learning

based algorithms, the method in this paper, although the processing efficiency is not optimal in individual cases, has some advantages in general. Of the four algorithms compared, the average time consumed by Projective Convolutional Network is 17.92s, 2.1 times the average processing time of our algorithm, Spectral Clustering is close to our method in processing speed and 1.08 times the average processing time of our algorithm.

On the other hand, in the quality of part model segmentation, we also made a comparison in this paper. For the examples used for analysis, we give the standard segmentation results by manual division, first we numbered each triangle mesh, then manually classify the triangle mesh in each boundary area. By dividing and classifying the numbered part model with the algorithm mentioned in this paper, comparing the achieved results with manual segmentation, calculating the number of triangular mesh on each model located in the correct region, and expressing the accuracy of each method segmentation result by the results similarity,
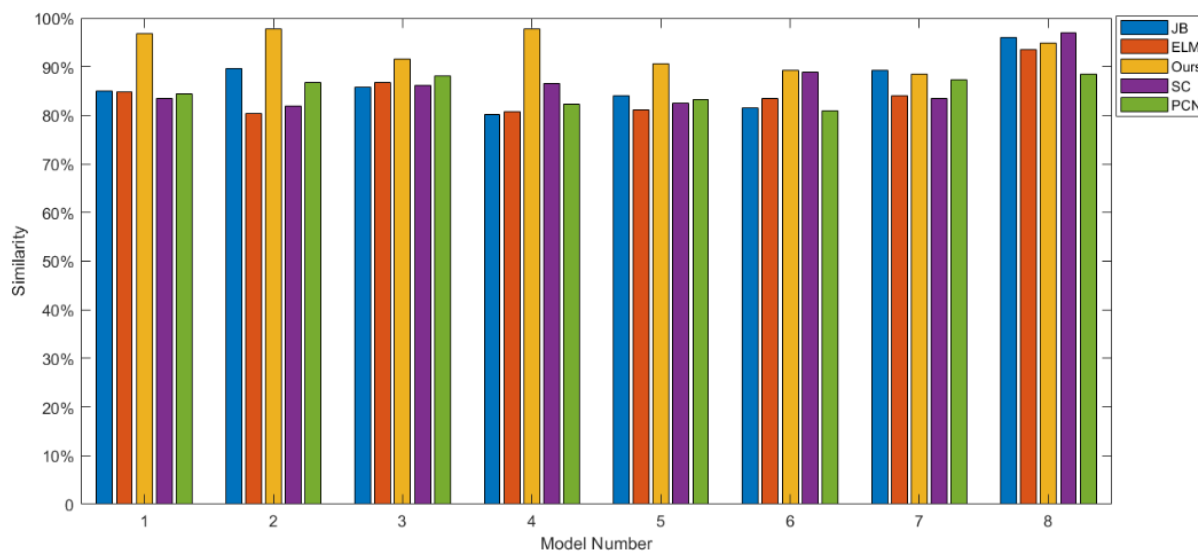
FIGURE 11. Comparison of the segmentation results quality about all the algorithm.

then we obtained the results as shown in Fig.11. It can be seen from the diagram that the method in this paper has some advantages in the accuracy of part mesh model segmentation, and when the model is relatively simple, the results of each algorithm segmentation have little difference, and they all have high accuracy.

VII. CONCLUSION

In this paper, a surface segmentation method of part mesh model for On-Machine Inspection is proposed, which aims to solve the problem that the geometric and topological information cannot be obtained when using the mesh model in the network environment. Based on the discrete curvature of each coordinate point on the part mesh model, this paper researched the characteristics of curvature distribution on the mesh model to screen the boundary points on the model, explores the extraction method of the model boundary line based on the maximum between-cluster variance, established the boundary matrix to describe the properties of each boundary on the model, and proposed a test method for boundary closure. Finally, the classification algorithm of the mesh surface in the boundary line is studied with the theory of region growth.

In the future work, we will aimed at the shortcomings of our method and try to improve it, starting from the following aspects. First, try to improve the threshold segmentation to achieve better and faster deviation of coordinate curvature values and model boundary lines, it helps to improve the accuracy of the final results. Secondly, we will study better boundary inspection methods, expand the scope for the usage of this method and enhance the rationality of the test results to obtain more realistic boundaries. Finally, we will study the efficient and fast classification method for large-scale

model and large-volume mesh model in order to improve the processing efficiency.

REFERENCES

[1] B. Li, P. Feng, L. Zeng, C. Xu, and J. Zhang, "Path planning method for on-machine inspection of aerospace structures based on adjacent feature graph," *Robot. Comput.-Integr. Manuf.*, vol. 54, pp. 17–34, Dec. 2018.

[2] C. Raibulet, F. Arcelli Fontana, and M. Zanoni, "Model-driven reverse engineering approaches: A systematic literature review," *IEEE Access*, vol. 5, pp. 14516–14542, 2017.

[3] R. S. V. Rodrigues, J. F. M. Morgado, and A. J. P. Gomes, "Part-based mesh segmentation: A survey," *Comput. Graph. Forum*, vol. 37, no. 6, pp. 235–274, Sep. 2018.

[4] F. Buonamici, R. Furferi, L. Governi, S. Lazzeri, K. S. McGreevy, M. Servi, E. Talanti, F. Uccheddu, and Y. Volpe, "A practical methodology for computer-aided design of custom 3D printable casts for wrist fractures," *Vis. Comput.*, vol. 36, no. 2, pp. 375–390, Feb. 2020.

[5] H. Zhang, C. Li, L. Gao, S. Li, and G. Wang, "Shape segmentation by hierarchical splat clustering," *Comput. Graph.*, vol. 51, pp. 136–145, Oct. 2015.

[6] M. Wencka and K. Walas, "Review of 3D objects segmentation methods," in *Advances in Intelligent Systems and Computing*, vol. 550. 2017, pp. 595–604.

[7] S. Mansouri and H. Ebrahimnezhad, "Segmentation-based semi-regular remeshing of 3D models using curvature-adapted subdivision surface fitting," *J. Visualizat.*, vol. 19, no. 1, pp. 141–155, Feb. 2016.

[8] V. A. A. Quirita, P. A. Diaz, R. Q. Feitosa, P. N. Happ, G. A. O. P. Costa, T. Klinger, and C. Heipke, "Metaheuristics for supervised parameter tuning of multiresolution segmentation," *IEEE Geosci. Remote Sens. Lett.*, vol. 13, no. 9, pp. 1364–1368, Sep. 2016.

[9] F. Yang, F. Zhou, R.-M. Wang, L. Liu, and X.-N. Luo, "A fast and efficient mesh segmentation method based on improved region growing," *Appl. Math.-A, J. Chin. Universities*, vol. 29, no. 4, pp. 468–480, Dec. 2014.

[10] B. Venu, V. R. Komma, and D. Srivastava, "STEP-based feature recognition system for B-spline surface features," *Int. J. Autom. Comput.*, vol. 15, no. 4, pp. 500–512, Aug. 2018.

[11] H. M. A. Hussein and H. M. Mousa, "Computer aided feature recognition in free form parts," in *Proc. 2nd Int. Conf. Sustain. Intell. Manuf. Green Design, Mater. Manuf. (SIM)*, 2013, pp. 239–244.

[12] V. B. Sunil and S. S. Pande, "Automatic recognition of features from freeform surface CAD models," *Comput.-Aided Des.*, vol. 40, no. 4, pp. 502–517, Apr. 2008.

[13] K. P. Siddappa and A. M. M. Salman, "A rule based method to auto-recognize fillet features of B-rep mill parts," *Eng. Appl. New Mater. Technol. Adv. Struct. Mater.*, vol. 85, pp. 105–114, Jan. 2018.

[14] H. Benhabiles, G. Lavoué, J.-P. Vandeborre, and M. Daoudi, "Learning boundary edges for 3D-mesh segmentation," *Comput. Graph. Forum*, vol. 30, no. 8, pp. 2170–2182, Dec. 2011.

[15] P. Theologou, I. Pratikakis, and T. Theoharis, "Unsupervised spectral mesh segmentation driven by heterogeneous graphs," *IEEE Trans. Pattern Anal. Mach. Intell.*, vol. 39, no. 2, pp. 397–410, Feb. 2017.

[16] L. P. Muraleedharan, S. S. Kannan, A. Karve, and R. Muthuganapathy, "Random cutting plane approach for identifying volumetric features in a CAD mesh model," *Comput. Graph. (Pergamon)*, vol. 70, pp. 51–61, Feb. 2018.

[17] T. Pin, Z. Bo, and Y. Zhen, "Segmentation and coding algorithm in 3D feature recognition," *Comput. Integr. Manuf. Syst.*, vol. 8, no. 10, pp. 813–818, 2002.

[18] S. Katz, G. Leifman, and A. Tal, "Mesh segmentation using feature point and core extraction," *Vis. Comput.*, vol. 21, nos. 8–10, pp. 649–658, Sep. 2005.

[19] D. D. Hoffman and W. A. Richards, "Parts of recognition," *Cognition*, vol. 18, nos. 1–3, pp. 65–96, 1984.

[20] O. K.-C. Au, C.-L. Tai, H.-K. Chu, D. Cohen-Or, and T.-Y. Lee, "Skeleton extraction by mesh contraction," *ACM Trans. Graph.*, vol. 27, no. 3, pp. 1–10, Aug. 2008.

[21] H. Zhang, C. Wu, J. Deng, Z. Liu, and Y. Yang, "A new two-stage mesh surface segmentation method," *Vis. Comput.*, vol. 34, no. 11, pp. 1597–1615, Nov. 2018.

[22] Z. Wu, Y. Wang, R. Shou, B. Chen, and X. Liu, "Unsupervised co-segmentation of 3D shapes via affinity aggregation spectral clustering," *Comput. Graph.*, vol. 37, no. 6, pp. 628–637, Oct. 2013.

[23] K. Saji, M. Umehara, and K. Yamada, "Coherent tangent bundles and Gauss–Bonnet formulas for wave fronts," *J. Geometric Anal.*, vol. 22, no. 2, pp. 383–409, 2012.

[24] L. Liu, Y. Sheng, G. Zhang, and H. Ugail, "Graph cut based mesh segmentation using feature points and geodesic distance," in *Proc. Int. Conf. Cyberworlds (CW)*, Oct. 2015, pp. 115–120.

[25] N. Dyn, K. Hormann, S.-J. Kim, and D. Levin, "Optimizing 3D triangulations using discrete curvature analysis," *Math. Methods Curves Surf.*, 2001, pp. 135–146.

[26] L. Qing, H. Tang, J.-N. Chi, Y.-Y. Xing, and H.-T. Li, "Gesture segmentation with improved maximum between-cluster variance algorithm," *Zidonghua Xuebao/Acta Automatica Sinica*, vol. 43, no. 4, pp. 528–537, 2017.

[27] Y. Peng, Y. Chen, and B. Huang, "Region segmentation for STL triangular mesh of CAD object," *Int. J. Sensor Netw.*, vol. 19, no. 1, pp. 62–68, 2015.

[28] Z. Xie, K. Xu, L. Liu, and Y. Xiong, "3D shape segmentation and labeling via extreme learning machine," *Comput. Graph. Forum*, vol. 33, no. 5, pp. 85–95, 2014.

[29] E. Kalogerakis, A. Hertzmann, and K. Singh, "Learning 3D mesh segmentation and labeling," *ACM Trans. Graph.*, vol. 29, no. 4, pp. 1–12, Jul. 2010.

[30] E. Kalogerakis, M. Averkiou, S. Maji, and S. Chaudhuri, "3D shape segmentation with projective convolutional networks," in *Proc. IEEE Conf. Comput. Vis. Pattern Recognit. (CVPR)*, Jul. 2017, pp. 6630–6639.

[31] R. Liu and H. Zhang, "Segmentation of 3D meshes through spectral clustering," in *Proc. 12th Pacific Conf. Comput. Graph. Appl. (PG)*, 2004, pp. 298–305.

BUYUN SHENG was born in Huarong, Hunan, China, in 1964. He received the B.S., M.S., and Ph.D. degrees in mechanical engineering from the Wuhan University of Technology, Wuhan, China, in 1985, 1988, and 2001, respectively.

He is currently a Professor with the School of Mechanical and Electronic Engineering, Wuhan University of Technology. He is the author of two books and more than 100 articles. His research interests include digital and intelligent manufacturing, cloud manufacturing and service, computer graphics, and CAD/CAPP/PDM.

HUI WANG was born in Nanchang, Jiangxi, China, in 1993. He received the B.S. degree in mechanical engineering from the Wuhan University of Technology, Wuhan, China, in 2015, where he is currently pursuing the Ph.D. degree.

His research interests include scheduling, digital manufacturing, and project management.

RUIPING LUO was born in Daye, Hubei, China, in 1993. He received the M.S. degree in mechanical engineering from the Wuhan University of Technology, Wuhan, China, in 2017, where he is currently pursuing the Ph.D. degree.

His research interests include PLM, workflow management, and digital manufacturing.

GAOCAI FU was born in Guangshui, Hubei, China, in 1989. He received the B.S. and M.S. degrees in mechanical engineering from the Wuhan University of Technology, Wuhan, China, in 2013 and 2016, respectively, where he is currently pursuing the Ph.D. degree.
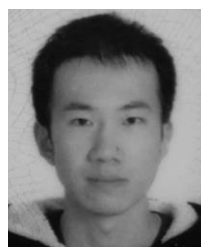
His research interests include CAD/CAPP/ PDM, intelligent manufacturing, and digital manufacturing.

XINCHENG LU was born in Guilin, Guangxi, China, in 1991. He received the M.S. degree in mechanical engineering from the Guilin University of Electronic Technology, Guilin, in 2018. He is currently pursuing the Ph.D. degree.

His research interests include digital manufacturing, intelligent manufacturing, and CAD.

QIBING LU was born in Gushi, Henan, China, in 1988. He received the B.S., M.S., and Ph.D. degrees in mechanical engineering from the Wuhan University of Technology, Wuhan, China, in 2009, 2011, and 2016, respectively. He is currently a Lecturer with the School of Mechanical and Electronic Engineering. He is also with the Hubei Digital Manufacturing Key Laboratory, Wuhan University of Technology. He has published more than ten journal articles and conference papers. His research interests include the Internet of Manufacturing Things and intelligent manufacturing.

● ● ●